INTERNATIONAL JOURNAL OF AUTOMOTIVE SCIENCE AND TECHNOLOGY

2022, VOL. 6, NO:4, 317-323 www.ijastech.org e-ISSN: 2587-0963

A Reliability-Enhanced Forming Grinding Method of Cylindrical Involute Gears for Electrical Vehicles

Zhi GENG[1*] and Gang LI[2]

0000-0002-4513-9984, 0000-0003-2793-4615

[1]*Shanghai Macrockets Technology Co., Ltd, Minhang, Shanghai, 201101, China*

[2]*Department of Mechanical Engineering, University of Maryland Baltimore County, Baltimore MD, 21250, United States*

Abstract

A new form-grinding method of cylindrical involute gears for electrical vehicles (EVs) is proposed to obtain stable contact performance of gear tooth surfaces and improve their reliability based on a predesigned controllable second-order transmission error function. The predesigned second-order transmission error function is assigned to a gear drive based on design specifications of EVs. Mathematical models of modified gear tooth surfaces of the gear pair can be obtained by the predesigned second-order transmission error function. Moreover, a section profile of a form-grinding wheel for cylindrical involute gears can be determined by a coordinate transformation matrix during form-grinding and settings of computer numerical control form-grinding programs for this active design method. This approach is ultimately conducted on three cylindrical involute gear pairs to demonstrate its feasibility and effectiveness.

Keywords Cylindrical involute gears; Second-order transmission error; Form-grinding; Electrical vehicles

Research Article

https://doi.org/10.30939/ijastech..1171720

Received 07.09.2022
Revised 18.10.2022
Accepted 26.10.2022

* Corresponding author
Zhi GENG
gengzhi_vali@163.com
Address: Shanghai Macrockets Technology Co., Ltd, Minhang, Shanghai, 201101, China
Tel: +86 138-1645-4123
Fax: +86 0539 5921380
Tel:+903122028653

1. Introduction

Electric vehicles (EVs) has become the main direction of automotive technology development because of its characteristics of high-energy efficiency, low emission and diversified energy source [1]. To achieve targets of high-efficiency and high-power of EVs, the integration of a high-speed motor and a gearboxes is a development trend of an electric drivetrain system [2,3]. A new drivetrain scheme of a two-speed planetary gearbox and a one-way clutch can well match with the high-speed motor. A vehicle transmission transmits the rotating power of the energy source, whether an electric motor or an internal combustion engine (ICE), through a set of gears to a differential, the unit that spins the wheels [4-6]. Any vehicle, ICEs or EVs, needs more torque than speed to propel the car from a dead stop, and more speed than torque once the vehicle already has forward momentum [7,8]. Comparing with traditional multi-speed gearboxes for ICEs, the two-speed gearbox is simplified but has a high requirement on its reliability [9]. The reliability performance of the two-speed planetary gearbox of the EV is closely related to the characteristics of transmission errors of its gear pairs [10].

Cylindrical involute gears, i.e., spur and helical ones, are widely used in gearboxes and planetary gear trains in many other industrial applications [11-13]. Evolution of the design and manufacture of such gears by hobbing, shaping, and grinding has been impressive. Geometry, design and manufacture of helical gears was the subject of research represented in the works [14-16] and many others. Generally, gears are manufactured via hobbing [17,18] or forming cutting [19-21] based on the theory of gearing. For some gears with special tooth profiles, e.g., concave-convex and spiral tooth profiles, their manufacturing methods and machine-tools are complex. Since meshing performances of these gears with special tooth profiles are highly sensitive to manufacturing errors [22,23], high manufacturing accuracy of gear machine-tools is required for these gears [24-27].

Transmission errors and contact patterns are two typical methods for meshing performances evaluation of gear systems [10,28,29]. A tooth profile modeling method was developed to improve accuracy of tooth contact analysis for gear tooth profiles [30]. Some other meshing performances, e.g., power losses, can also be evaluated based tooth contact analysis [31-33]. Since these gears have convex-concave tooth profiles, they cannot be manufactured via standard gear manufacturing methods. During a manufacture

in this way, for each of the gear modules and the radius of curvature, a different blade size and gear holder is needed. However, it's clear that these gears have many advantages, if they can be produced sufficiently in the industry [34,35]. Since these gears have better load-bearing capabilities, have a balancing feature for the axial forces, quiet operation feature and their lubrication characteristics is better than herringbone gears and spur gears [36-38]. It's noteworthy that there are number of studies carried out recently in relation to these gears [39,40]. Many applications, e.g., automobile [41,42] and tunnel boring machines [43,44] require high reliability of gearboxes.

Application of modern CNC for gear form grinding methods is introduced new concepts in design and formed of involute gears with modifications. The study describes a new reliability-enhanced form grinding method based on a predesigned second-order transmission error function. The proposed method is based on the kinematical modeling of the basic machine settings and motions of a virtual generating rack cutter. This work focus on the design of gear drives with reduced noise is based on application of a predesigned parabolic function of transmission errors.

2. Functions of Second-Order Transmission Errors

It has been already recognized by researchers that the main source of vibration and noise are transmission errors [1-3]. Reduction of transmission errors and controlling the shape of the function of transmission errors are able to improve the dynamic performance of gear meshing and reduce vibration.

Conventionally, the function of transmission errors can be represented as

$$\Delta\varphi_2 = (\varphi_2 - \varphi_2^{(0)}) - \frac{z_1}{z_2}(\varphi_1 - \varphi_1^{(0)}) \tag{1}$$

where φ_1 and φ_2 are the real rotation angles of the driving gear and driven gear, respectively, z_1 and z_2 are the number of teeth for the driving gear and driven gear, respectively and $\varphi 1(0)$ and $\varphi 2(0)$ are the theoretical rotation angles for the driving gear and driven gear, respectively.

Eq. (1) is a periodic function with period $T=2\pi/z1$. A predesigned second-order parabolic function of transmission error is applied to reduce or eliminate gear noise and increase gear strength for forming grinding method of involute gears. As shown in Figure.1, the second-order polynomial function is represented as

$$\Delta\varphi_2 = b_0 + b_1\varphi_1 + b_2\varphi_1^2 = \boldsymbol{X}\boldsymbol{Y}^{\mathrm{T}} \tag{2}$$

where $\boldsymbol{X} = [b0\ b1\ b2]^{\mathrm{T}}$ and $\boldsymbol{Y} = [1\ \varphi 1\ \varphi 12]^{\mathrm{T}}$. As shown in Figure 1, the geometry of the second-order polynomial function is represented as

$$\varphi_1 = -\delta + T/2, \quad \Delta\varphi_2 = -\varepsilon \tag{3}$$

$$\varphi_1 = -\delta - T/2, \quad \Delta\varphi_2 = -\varepsilon \tag{4}$$

$$\varphi_1 = -\delta, \quad \Delta\varphi_2 = 0 \tag{5}$$

where ε and δ are parameters that can be used to control the shape of the second-order polynomial function. Equations (3) - (5) are applied to control the geometric characters of the second-order polynomial function of transmission error $\Delta\varphi_2$. And Eqs. (3)-(5) can be represented in the following matrix form:

$$\boldsymbol{A}\boldsymbol{X} = \boldsymbol{B} \tag{6}$$

where

$$\boldsymbol{A} = \begin{bmatrix} 1 & (-\delta + T/2) & (-\delta + T/2)^2 \\ 1 & (-\delta - T/2) & (-\delta - T/2)^2 \\ 1 & -\delta & \delta^2 \end{bmatrix}, \quad \boldsymbol{B} = \begin{bmatrix} -\varepsilon \\ -\varepsilon \\ 0 \end{bmatrix}$$

The coefficient vector $\boldsymbol{X}$ can be solved as follows:

$$\boldsymbol{X} = \boldsymbol{A}^{-1}\boldsymbol{B} \tag{7}$$

Substituting Eq. (7) into Eq. (2) yields

$$\Delta\varphi_2 = \boldsymbol{A}^{-1}\boldsymbol{B}\boldsymbol{Y}^{\mathrm{T}} \tag{8}$$

By substituting Eq. (8) into Eq. (1), the rotation angle of the driven gear φ_2 can be represented as

$$\varphi_2 = \boldsymbol{A}^{-1}\boldsymbol{B}\boldsymbol{Y}^{\mathrm{T}} + \frac{z_1}{z_2}\varphi_1 \tag{9}$$

Equation (9) is the constraint equation of the rotation angle of the driving gear φ_1 and the rotation angle of the driven gear φ_2. As long as the rotation angles φ_1 and φ_2 are restrained by Eq. (9), the gear pair is able to reproduce the predesigned second-order polynomial function of transmission error $\Delta\varphi_2$.

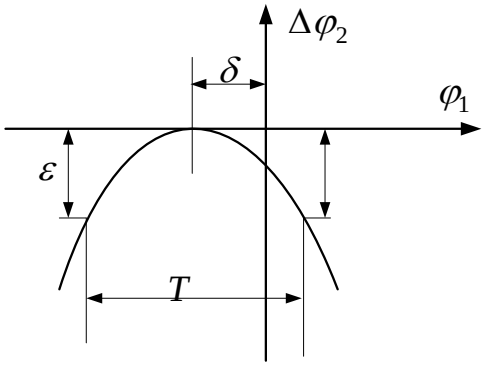

Fig. 1. The second-order function of transmission error.

3. Model of the Hypothetical Generator

3.1 Pothetical generating rack cutter

Based on the theory of gearing, the involute tooth face can be generated by a rack cutter with a planar tooth face. As shown in Figure 2, the generating rack cutter translates horizontally when the generated gear rotates about a fixed axis. The reference circle of the gear rolls without sliding with respect to the pitch line of the rack cutter. Coordinate systems $S_a(x_a, y_a, z_a)$ and $S_b(x_b, y_b, z_b)$ are applied to connect rigidly to the generating rack cutter. $S_c(x_c, y_c, z_c)$ is the movable coordinate system. The position vector and the unit normal vector of the hypothetical generating rack cutter are represented as follows:

$$\boldsymbol{r}_c(u_c,l_c)=\begin{bmatrix} u_c\cos\alpha_n+a_c{u_c}^2\sin\alpha_n-d_p\cos\alpha_n \\ \left(u_c\sin\alpha_n-a_c{u_c}^2\cos\alpha_n+a_m-d_p\sin\alpha_n\right)\cos\beta+l_c\sin\beta \\ \left(-u_c\sin\alpha_n+a_c{u_c}^2\cos\alpha_n-a_m+d_p\sin\alpha_n\right)\sin\beta+l_c\cos\beta \end{bmatrix} \quad (10)$$

$$\boldsymbol{n}_c(u_c)=\begin{bmatrix} \sin\alpha_n-2a_cu_c\cos\alpha_n \\ -\left(\cos\alpha_n+2a_cu_c\sin\alpha_n\right)\cos\beta \\ \left(\cos\alpha_n+2a_cu_c\sin\alpha_n\right)\sin\beta \end{bmatrix} \quad (11)$$

where u_c and l_c are surface coordinates of the generating rack cutter blade, β is the spiral angle, α_n is the pressure angle, a_m is half of the face width, d_p is position of the parabolic pole, and a_c is parabolic modification coefficient of the cutter tooth profile.

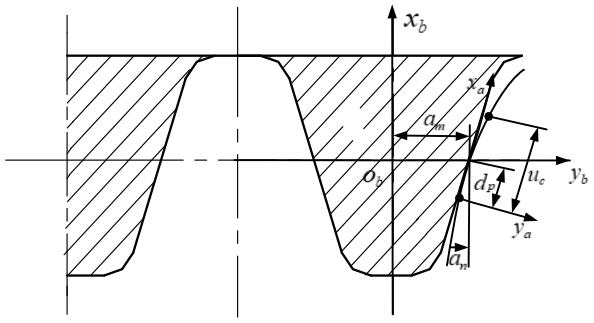

(a)

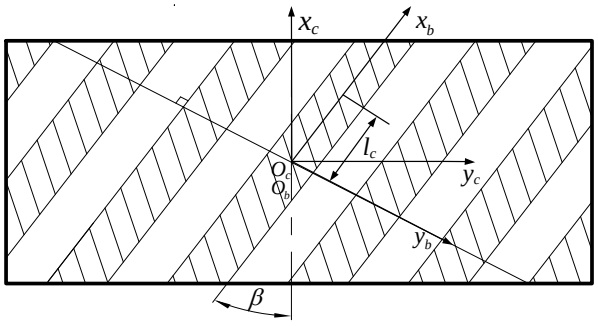

(b)

Fig. 2. Coordinate systems of the hypothetical generating rack cutter.

3.2 Mathematical model of the tooth surface of the driving gear

A general mathematical model for the generation of tooth surfaces of the driving gear is adopted as shown in Figure 3. Coordinate systems $S_m(x_m, y_m, z_m)$ and $S_p(x_p, y_p, z_p)$ are rigidly attached to work piece that is the driving gear in this study. In the coordinate system S_p, the driving gear rotates φ_1, the generating rack cutter moves $r_1\varphi_1$, where r_1 is the radius of base circle of the driving gear.

Based on the theory of gearing, the necessary condition for the existence of an envelope to the rack cutter surface can be determined as

$$\frac{X_c-x_c}{\boldsymbol{n}_{cx}}=\frac{Y_c-y_c}{\boldsymbol{n}_{cy}}=\frac{Z_c-z_c}{\boldsymbol{n}_{cz}} \quad (12)$$

where X_c, Y_c, and Z_c are coordinates of the axis I-I in coordinate system S_c on the generating rack cutter, x_c, y_c, and z_c are coordinates of the contact point in coordinate system S_c, and $\boldsymbol{n}_{cx}$, $\boldsymbol{n}_{cy}$, and $\boldsymbol{n}_{cz}$ are normal vectors of the contact point.

The surface Σ_p of the generated driving gear tooth surface is represented as follows

$$\boldsymbol{r}_p(u_c,l_c)=\boldsymbol{M}_{pc}(\varphi_1)\boldsymbol{r}_c(u_c,l_c) \quad (13)$$

$$\boldsymbol{n}_p(u_c,l_c)=\boldsymbol{L}_{pc}(\varphi_1)\boldsymbol{n}_c(u_c,l_c) \quad (14)$$

where $\boldsymbol{M}_{pc}$ and $\boldsymbol{L}_{pc}$ are transformation matrixes from coordinate S_c to S_p.

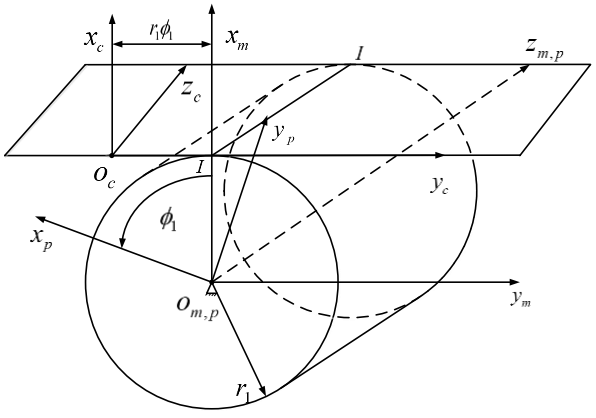

Fig. 3. The coordinate systems of the driving gear.

3.3 Mathematical model of the tooth surface of the driven gear

When the driving gear rotates with the angular ϕ_1, the driven gear is constraint to rotate with the angular ϕ_2. ϕ_1 and ϕ_2 are restrained by Eq.(9).

As shown in Figure 4, the tooth surface Σ_p of the driving gear is regarded as the generating surface of the tooth surface Σ_g of the driven gear. In S_g, Σ_p forms a family of surfaces the position vector of which can be determined by

$$\begin{cases} \mathrm{r}_g\left(u_c,\phi_2\right)=\mathrm{M}_{gp}\left(\phi_1\right)\mathrm{r}_p\left(u_c,l_c\right) \\ \mathrm{n}_g\left(u_c,\phi_2\right)=\mathrm{L}_{gp}\left(\phi_1\right)\mathrm{n}_p\left(u_c,l_c\right) \end{cases} \quad (15)$$

where $\boldsymbol{M}_{gp}$ and $\boldsymbol{L}_{gp}$ are transformation matrixes from coordinate S_p to S_g.

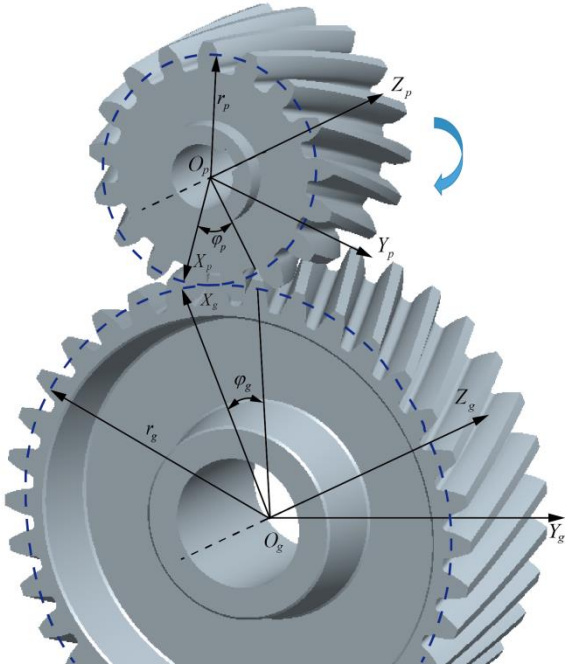

Fig. 4. The coordinate systems of the driven gear.

4. Determination of the Grinding Wheel with the Second Order Transmission Error

In the form grinding progress of helical gears, the contact line between the surface Σ_w of the grinding wheel and the surface of the workpiece (the gear) is a space spiral curve. The formation of the forming grinding wheel surface Σ_w is achieved by the contact line rotary around the grinding wheel axis. Therefore, according to the relationship of the relative position and movement between the grinding wheel and the gear, the coordinate system $S_w(x_w, y_w, z_w)$ is established, as shown in Figure 5.

4.1 Coordinate systems of the form grinding wheel

As shown in Figure 5, coordinate systems $S_w(x_w, y_w, z_w)$ and $S_g(x_g, y_g, z_g)$ rigidly connect the form grinding wheel and the driven gear, respectively; Z_g-axis is the rotation axis of the driven gear, and Z_w-axis is the rotation axis of the from grinding wheel, a is the center distance, Σ is the included angle between Z_g-axis and Z_w-axis. The transformation relationship between coordinate S_g and S_w is represented as

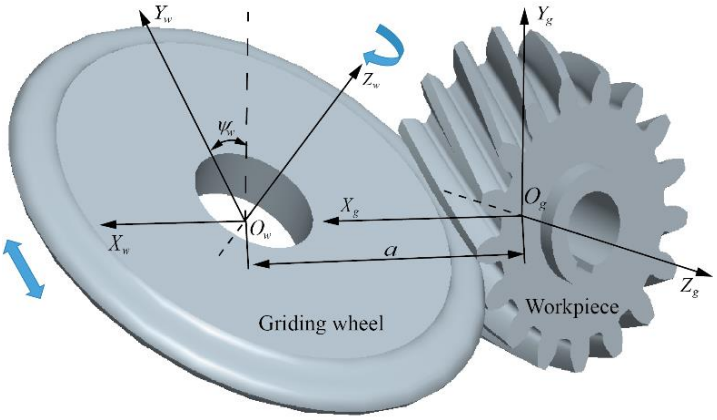

Fig. 5. Coordinate systems of the form grinding wheel.

$$\begin{cases} X_w = a - X_g \\ Y_w = -Y_g \cos\Sigma - Z_g \sin\Sigma \\ Z_w = -Y_g \sin\Sigma + Z_g \cos\Sigma \end{cases} \tag{16}$$

4.2 The mathematical model of the form grinding wheel

The position that the helicoid grinding wheel surface and the workpiece tangent contact is along the contact line. Therefore, based on the theory of gearing, the necessary constraint to normal vector $\boldsymbol{n_g}(u_c, \phi_2)$ and the relative velocity $\boldsymbol{v_{gw}}$ is

$$\boldsymbol{n}_g(u_c, \phi_2) \cdot \mathrm{v}_{gw} = 0 \tag{17}$$

where

$$\boldsymbol{n}_g(u_c, \phi_2) = \begin{bmatrix} \boldsymbol{n}_{xg} \\ \boldsymbol{n}_{yg} \\ \boldsymbol{n}_{zg} \end{bmatrix} = \boldsymbol{L}_{pc}(\phi_1) \begin{bmatrix} \sin\alpha_n \\ -\cos\alpha_n \cos\beta \\ \cos\alpha_n \sin\beta \end{bmatrix} \tag{18}$$

In the coordinate system S_w, projections of the angular velocity $\boldsymbol{\omega}$ of form grinding wheel rotation on coordinate axis are

$$\omega = \begin{pmatrix} 0 & -\omega\sin\Sigma & \omega\cos\Sigma \end{pmatrix}^{\mathrm{T}} \tag{19}$$

With Eqs. (16)-(19), one has

$$(Z_g + Y_g \cdot \cot\Sigma) \cdot \mathrm{n}_{xg} - (X_g - a) \cdot (\mathrm{n}_{yg} \cdot \cot\Sigma + \mathrm{n}_{zg}) = 0 \tag{20}$$

There are two parameters in Eq.(20), u_c and ϕ_2. Based on Newton-Raphson method, we generate the discrete points recursively by choosing step size Δu_c, $\Delta\phi_2$ respectively. The section profile of the form grinding wheel is formed by these discrete points, as shown in Figure 6.

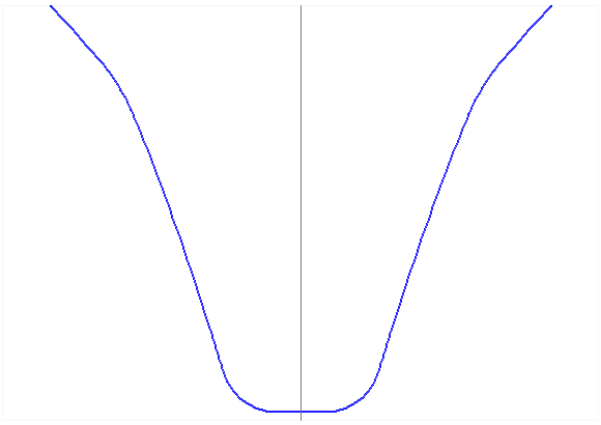

Fig. 6. Section profile of the form grinding wheel.

5. Case Study

In order to verify the consistency between actual transmission error and predesigned transmission error of the form grinding gear. Three examples of numerical analysis are shown in Table 1.

Table 1. Settings of parameters for numerical analysis.

Parameters	Example 1	Example 2	Example 3
z_1	31	31	31
z_2	81	81	81
m_n / (mm)	3	3	3
α_n / (°)	20	20	20
β / (°)	15	15	15
ε / (″)	3.873	2.502	2.476
T / (rad)	0.203	0.203	0.203
δ / (rad)	0.000	0.000	0.000

Table 2. The modification coefficients

Parameters	a_{c1}	a_{c2}
Case 1	0.002	0.000
Case 2	0.0025	-0.0015
Case 3	0.002	-0.001

Based on second-order predesigned of involute gear transmission error method, the modification coefficients of the numerical analysis can be obtained, as shown in Table 2. And according to the forming algorithm for section profile of grinding wheel, we can complete forming grinding process of examples in Table 1, as shown in Figure 7. Some machine-tool settings of form-grinding tests are listed in Table 3.

Table 3. Machine-tool settings of form-grinding tests

Parameters	Values
Spindle speed / (rad/min)	4200
Grinding linear velocity / (m/s)	35
Feed velocity / (m/s)	0.02

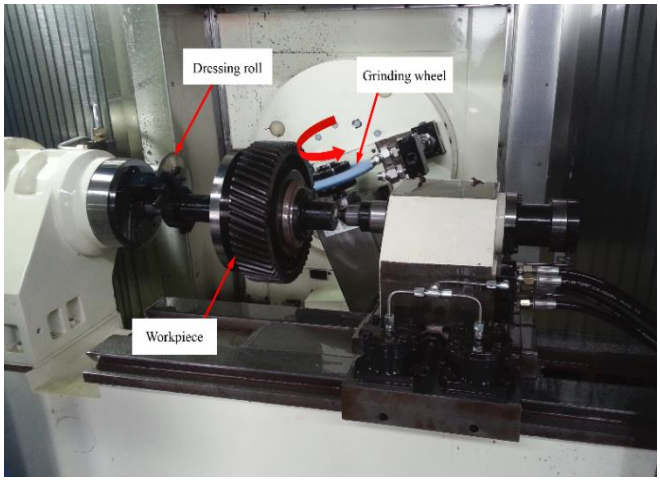

Fig. 7. The form grinding testing.

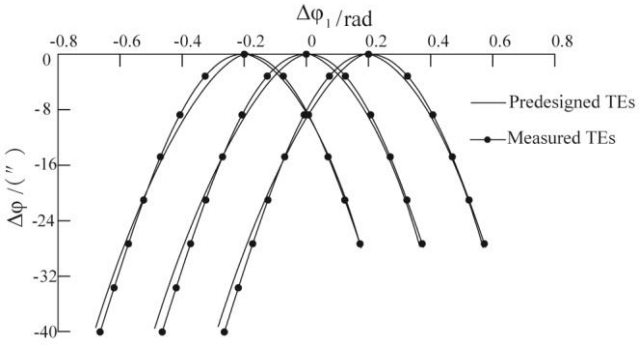

Fig. 8. The comparison for transmission errors of Case 1.

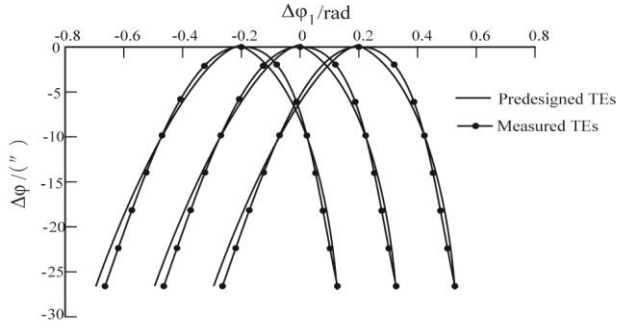

Fig. 9. The comparison for transmission errors of Case 2.

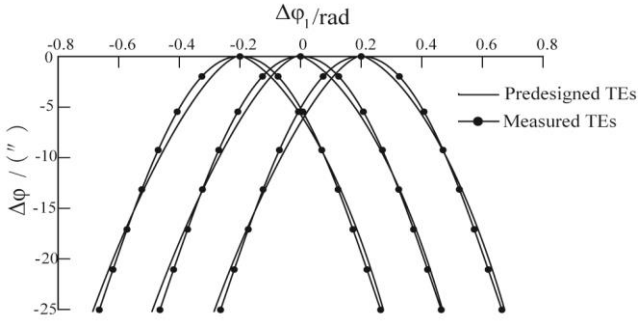

Fig. 10. The comparison for transmission errors of Case 3.

According to the above method, the numerical analysis results are shown in Figures 8-10. The maximum error among the predesigned transmission error curve and the numerical analysis results is 1.19 ". Through the predesigned transmission error, we can realize to contain complex modification request of involute gear design, and achieving the precontrol on its dynamic performance.

Furthermore, local geometry parameters of measured TE curves are in general accordance with predesigned ones. For instance, the amplitude ε of the predesigned TE function curve is 0.5", and that of the measured TE curve in Case 1 in Fig. 8 is 0.83". Amplitudes of measured TE curves in Cases 2 and 3 in Figs. 9 and 10 are 0.74" and 0.68", respectively. Amplitudes of measured TE curves in Cases 2 and 3 are close to the predesigned one; the corresponding errors are -0.7" and -0.82", respectively. While the error of the amplitude of measured TE curves in Case 1 is 0.39", it is still within an acceptable level.

Results of form-grinding tests and tooth surface measurement demonstrate that this form-grinding method is effective and accurate for manufacturing modified tooth surfaces calculated by a predesigned fourth-order TE function. Hence, it can be concluded that actual TE of modified tooth surfaces can be controlled by the predesigned TE function. The method can provide guidance on optimal design of a gear drive.

6. Conclusions

Theoretically, the proposed reliability-enhanced form grinding method for cylindrical involute gears based on the predesigned second-order transmission error is not limited to the involute tooth profile, and is applicable to all types of gears. Because of the light load cases can reflect more gear noise problems. Especially, involute gears with time-varying meshing stiffness are difficult to adjust amount of modification. Therefore, on the basis of the obtained results, the following conclusions can be made:

1. By the predesigned second-order transmission error function, it is realized with very complex modification conditions forming grinding involute gear tooth modification process parameters adjustment.

2. Through a hypothetical generative algorithm by a generating rack, the mathematical model of the section profile of the form grinding wheel is realized based on the second-order transmission error.

3. The advantage of application of a predesigned parabolic function of transmission errors is confirmed by numerical analysis of the transmission errors caused by typical function of transmission errors of gear drives. This can be achieved ahead of the manufacturing process of a designed gear drive.

4. The reliability of transmission errors of gearboxes can be improved based on the proposed form-grinding method with the predesigned second-order transmission error function.

Acknowledgment

The authors are grateful for the financial support from the Shanghai Education Commission, Science and Technology Innovation Projects, Grant No. 11CXY45.

Conflict of Interest Statement

The authors declare that there is no conflict of interest in the study.

CRediT Author Statement

Zhi GENG: Conceptualization, Writing-original draft, Data curation, Software.
Gang LI: Conceptualization, Supervision, Writing-review&editing, Validation.

References

[1] Chen LL, Zhang H, Ni F. Present situation and development trend for construction of electric vehicle energy supply infrastructure. Power Syst Technol. 2011;35(14):11–17.

[2] Geng Z, Li G. Optimal clutch control of a one-way clutch assistant transmission for electrical vehicles. Int J Auto Sci Tech. 2022;6(3):257-264.

[3] Lu TL, Dai F, Zhang JW, Wu MX. Optimal control of dry clutch engagement based on the driver's starting intentions. Proc Instn Mech Eng, Part D: J Automob Eng. 2012;226(8):1048-1057.

[4] Di X, Huang Y, Ge Y, Li G, Hu M. Fuzzy-PID speed control of diesel engine based on load estimation. SAE Int J Engines. 2015;8(4):1669-1677.

[5] Huang Y, Wan G, Cui T, Li G. A study on engine control strategy for gear shifting of AMT. Automotive Engineering. 2012;34(3):245-248.

[6] Jiang D, Huang Y, Li G, Hao D, Zuo Z. Design of a speed tracking controller for heavy-duty vehicles with an all-speed governor based on a model predictive control strategy. Int J Engine Res. 2017;18(9):930-940.

[7] Li G, Zhu WD. Experimental investigation on control of an infinitely variable transmission system for tidal current energy converters. IEEE/ASME Trans Mechatron. 2021; 26(4):1960-1967.

[8] Li G, Zhu WD. Theoretical and experimental investigation on an integral time-delay feedback control combined with a closed-loop control for an infinitely variable transmission system. Mech Mach Theory. 2021;164:104410.

[9] Li X, Li G, Ren J, Li W. Numerical simulation of helical gear tooth root crack initiation life of high-speed EMUs. China Mech Eng. 2018;29(09):1017-1024.

[10] Wang ZH, Wang J, Wang QL, Li G. Transmission error of spiral bevel gear based on finite element method. J of Vib Shock. 2014;33(14):165-170.

[11] Hu YH, Li G, Zhu WD, Cui JK. An elastic transmission error compensation method for rotary vector speed reducers based on error sensitivity analysis. Appl Sci. 2020;10(2):481.

[12] Yan J, Li G, Liu K. Development trend of wind power technology. Int J Adv Eng Res Sci. 2020;7(6):124-132.

[13]Li G, Zhu WD. Time-delay closed-loop control of an infinitely variable transmission system for tidal current energy converters. Renew Energy. 2022;189:1120-1132.

[14]Li G. Design and modeling of an impulse continuously variable transmission with a rotational swashplate. Int J Auto Sci Tech. 2020;4(4):307-313.

[15]Xu M, Zhang X, Hu G, Li G. The structure design and flow field simulation of a fire water monitor driven by worm gear with bevel gear. Mach Tool & Hydra. 2016;6:57-61.

[16]Gu KL, Wang ZH, Li G, Liu XR. Optimization of geometric parameters of the straight conjugate internal gear pump based on GA. Elec Sci Tech, 2017;30(6):39-42.

[17]Zhang XL, Wang ZH, Li G. Research on virtual hobbing simulation and study of tooth surface accuracy of involute helical gears. Appl Mech Mater. 2012;155:601-605.

[18]Wang ZH, Li G, Zhang XL, Li KS. Study on the virtual hobbing simulation and tooth surface accuracy of the entirety of involute helical gears. J Mech Trans. 2012;36(8): 9-13.

[19]Li G, Wang ZH, Zhu WD, Kubo A. A function-oriented active form-grinding method for cylindrical gears based on error sensitivity. Int J Adv Manuf Tech. 2017;92(5-8):3019-3031.

[20]Wang ZH, Zhu WM, Li G, Geng Z. Optimization of contact line for form-grinding modified helical gears based on neural network. China Mech Eng. 2014;25(12):1665-1671.

[21]Li G. An active forming grinding method for cylindrical involute gears based on a second-order transmission error model. SCIREA J Mech Eng. 2019;2(1):1-14.

[22]Li G, Zhu WD. An active ease-off topography modification approach for hypoid pinions based on a modified error sensitivity analysis method. ASME J Mech Des. 2019;141(9):093302.

[23]Li G, Wang ZH, Kubo A. Error-sensitivity analysis for hypoid gears using a real tooth surface contact model. Proc Instn Mech Eng, Part C: J Mech Eng Sci. 2017;231(3):507-521.

[24]Zhang WX, Wang ZH, Liu XR, Li G, Wan PL, Wang W. Research on optimization of temperature measuring point and thermal error prediction method of CNC machine tools. J Shaanxi University of Tech (Na Sci Ed). 2017; 33(3):18-24.

[25]Wang ZH, Cao H, Li G, Liu XR. Compensation of the radial error of measuring head based on forming grinding machine. J Mech Trans. 2017;41(3):143-146.

[26]Wang ZH, Song XM, He WM, Li G, Zhu WM, Geng Z. Tooth surface model construction and error evaluation for tooth-trace modification of helical gear by form grinding. China Mech Eng. 2015;26(21):2841-2847.

[27]Li G, Wang ZH, Kubo A. Tooth contact analysis of spiral bevel gears based on digital real tooth surfaces. Chin J Mech Eng. 2014;50(15):1-11.

[28]Wang ZH, Wang J, Ma PC, Li G. Dynamic transmission error analysis of spiral bevel gears with actual tooth surfaces. J Vib Shock. 2014;33(15):138-143.

[29]Li G, Wang ZH, Kubo A. Tooth contact analysis of spiral bevel gears based on digital real tooth surfaces. Chin J Mech Eng. 2014;50(15):1-11.

[30]Li G, Wang ZH, Kubo A. The modeling approach of digital real tooth surfaces of hypoid gears based on non-geometric-feature segmentation and interpolation algorithm. Int J Prec Eng Manuf. 2016;17(3):281-292.

[31]Li G, Zhu WD. Design and power loss evaluation of a noncircular gear pair for an infinitely variable transmission. Mech Mach Theory. 2021;156:104137.

[32]Wei XT, Zhu JP, Li G. Automatic NC Programming for chamfering addendum of spiral bevel gear based on UG/Open. Appl Mech Mater. 2013;365:950-954

[33]Li G, Geng Z. Gear bending stress analysis of automatic transmissions with different fillet curves. Int J Auto Sci Tech. 2021;5(2):99-105.

[34]Huang DQ, Wang ZH, Li G, Zhu WD. Conjugate approach for hypoid gears frictional loss comparison between different roughness patterns under mixed elastohydrodynamic lubrication regime. Tribo Int. 2019;140:105884.

[35]Li G, Wang ZH, Zhu WD. Prediction of surface wear of involute gears based on a modified fractal method. ASME J Tribo. 2019;141(3):031603.

[36]Wu J, Wang ZH, Li G. Study on crack propagation characteristics and remaining life of helical gear. J Mech Trans. 2014;38(12):1-4.

[37]Li G, Wang ZH, Geng Z, Zhu WM. Modeling approach of digital real tooth surfaces of hypoid gears based on non-geometric-feature segmentation and interpolation algorithm. Chin J Mech Eng. 2015;51(7):77-84.

[38]Li G, Geng Z. Tooth contact analysis of herringbone rack gears of an impulse continuously variable transmission. Int J Auto Sci Tech. 2021;5(1):52-57.

[39]Wang ZH, Yuan KK, Li G. Optimization identification for dynamic characteristics parameters of sliding joints based on response surface methodology. China Mech Eng. 2016;27(5):622-626.

[40]Hu YH, Li G, Hu AM. Iterative optimization of orbital dynamics based on model prediction. Front Arti Intel App. 2019;320:76-86.

[41]Wan GQ, Huang Y, Zhang FJ, Li G. Integrated powertrain control for gear shifting. Appl Mech Mater. 2012;148: 725-730.

[42]Wei XT, Zhu JP, Li G. Automatic NC programming for chamfering addendum of spiral bevel gear based on UG/Open. Appl Mech Mater. 2013; 365, 950-954.

[43]Li G, Chen YD, Wang B, Wang WS. Dynamics simulation of a six-DOF tunnel segment erector for tunnel boring machine based on virtual prototype. Appl Mech Mater. 2013; 251, 231-234.

[44]Li G, Wang B, Chen YD, Wang WS. Numerical simulation of the rock fragmentation process induced by TBM cutters. Appl Mech Mater. 2013; 249, 1069-1072.